SECURITY INFORMATION

~~CONFIDENTIAL~~

Copy 5
RM L52D24b

NACA RM L52D24b

JUL 10 1952

NACA

RESEARCH MEMORANDUM

RESULTS OF TWO EXPERIMENTS ON FLUTTER OF HIGH-ASPECT-RATIO SWEPT WINGS IN THE TRANSONIC SPEED RANGE

By W. T. Lauten, Jr., and Burke R. O'Kelly

Langley Aeronautical Laboratory
Langley Field, Va.

CLASSIFICATION CANCELLED

Authority NACA Res. 685 Date 4/6/56
RN 99
By mxa 5/4/56 Sec

CLASSIFIED DOCUMENT

This material contains information affecting the National Defense of the United States within the meaning of the espionage laws, Title 18, U.S.C., Secs. 793 and 794, the transmission or revelation of which in any manner to an unauthorized person is prohibited by law.

NATIONAL ADVISORY COMMITTEE FOR AERONAUTICS

WASHINGTON

July 3, 1952

~~CONFIDENTIAL~~

NACA LIBRARY
LANGLEY AERONAUTICAL LABORATORY
Langley Field, Va.

NASA Technical Library
3 1176 01436 4633

NATIONAL ADVISORY COMMITTEE FOR AERONAUTICS

RESEARCH MEMORANDUM

RESULTS OF TWO EXPERIMENTS ON FLUTTER OF HIGH-ASPECT-RATIO SWEPT WINGS IN THE TRANSONIC SPEED RANGE

By W. T. Lauten, Jr., and Burke R. O'Kelly

SUMMARY

Flutter data obtained by use of rocket-propelled vehicles in the transonic speed range for two pairs of high-aspect-ratio swept wings are presented herein. Two wings, swept 45°, fluttered at a Mach number of 0.89 and the other two wings, swept 60°, fluttered at a Mach number of 1.09.

A reference flutter speed was calculated by means of a theory which includes effects of mode shape and sweep and involves the use of two-dimensional flutter derivatives based on flow normal to the wing. The agreement between the calculated and measured flutter speeds was very good, the experimental values being slightly higher in each case. The closeness of the agreement indicates that the method of calculation gives usable results in the transonic speed range for swept wings of high aspect ratio, provided that the normal-flow Mach number is sufficiently subsonic. A comparison of the test results with previous experiments on straight wings of comparable aspect ratio indicates that the turn-up of the curve of flutter-speed coefficient against Mach number lies at higher Mach numbers for swept wings than for the unswept wings.

INTRODUCTION

The effect of sweep on the bending-torsion flutter characteristics of wings is being investigated by the National Advisory Committee for Aeronautics by various methods, including free-flight tests of rocket-propelled vehicles and freely-falling bodies, wind-tunnel investigations, and theoretical studies (refs. 1 to 4). For some tests of swept wings of low aspect ratio (refs. 1 and 3) it has been indicated that the transonic region was the critical one; that is, that the turn-up of the curve of flutter-speed coefficient against Mach number would usually take place

in that region. It was known, however, that exceptions to these results did exist.

In order to extend the work reported in references 1 and 3 to higher aspect ratios, the two tests reported herein were performed. Since the primary objective of the tests was to investigate effects of sweep on the flutter of high-aspect-ratio wings in the transonic speed range, one pair of wings was swept 45° and the other pair was swept 60°. Both pairs were constructed with the relatively high length-to-root-chord ratio of 5.66, giving aspect ratios of 8.01 and 4.25 for the 45° and 60° wings, respectively. In order to simulate more closely the wings which are being considered for transonic bombers, the wings were tapered.

SYMBOLS

A	aspect ratio (including body intercept)
a	nondimensional wing-elastic-axis position measured from midchord, positive rearward, $\frac{2x_o}{100} - 1$
$a + x_\alpha$	nondimensional wing center of gravity measured from midchord, positive rearward, $\frac{2x_1}{100} - 1$
b	semichord of test wing normal to quarter-chord line, ft
F	calculated mode shape, $\frac{\text{Displacement of any spanwise section}}{\text{Displacement of tip}}$
f	frequency, cps
g	acceleration due to gravity, 32.2 ft/sec^2
I_α	polar mass moment of inertia about elastic axis per unit length, ft-lb-sec^2/ft
μ	mass ratio, $m/\pi\rho b^2$
l	exposed length of wing, measured along quarter chord, in.
Λ	sweepback, deg
λ	taper ratio of exposed wing panel

[redacted]

M	Mach number
m	mass of wing per unit length, slugs/ft
ρ	air density, slugs/cu ft
q	free-stream dynamic pressure, lb/sq ft
r_α^2	square of nondimensional radius of gyration about the elastic axis, I_α/mb^2
t	time, sec
V	flutter velocity, fps
x_o	distance of elastic axis of wing section behind leading edge, measured perpendicular to the quarter-chord line, percent chord
x_1	distance of center of gravity of wing section behind leading edge, measured perpendicular to the quarter chord line, percent chord

Subscripts:

e	experimental values obtained at the start of flutter
R	calculated values based on two-dimensional incompressible-flow theory, reference 4
h_1	first bending
h_2	second bending
α_1	first torsion

MODELS AND INSTRUMENTATION

Test Vehicle

The flutter test vehicle, as shown in figures 1 and 2, was essentially an airplane configuration with four tail surfaces to provide stability in pitch and yaw. In order to remove the tail surfaces as much as possible from the downwash field of the test wings for the

near-zero angle-of-attack condition, they were interdigitated 45° with respect to the test wings. The origin of the longitudinal coordinate system in figure 1 is located where the nose of the rocket would come to a point if the angle-of-attack boom were not attached. It may be seen in figure 2 that model 606 carried 45° swept wings and that model 607 carried 60° swept wings. An aluminum-alloy casting was used to provide both a rigid mounting for the wings and a thrusting surface for the 5-inch cordite rocket motor. This casting was designed with long slots on each side so that wings of various sizes and plan forms could be mounted on the model with the mean aerodynamic chord of the wings in the desired location relative to the center of gravity of the model. The complete model without fuel weighed 98.3 pounds, the fuel weighed 26 pounds, and the moment of inertia in pitch, when loaded, was 9.75 slug-feet^2.

In order to avoid excessive accelerations during that portion of the flight where flutter was expected the models were designed to be accelerated by boosters of various sizes up to the desired speed range and, after booster separation, a rocket motor in the model propelled it through this range at a relatively low acceleration. This arrangement resulted in a test range of Mach numbers for model 606 from 0.6 to approximately 1.2 and for model 607 from 0.9 to approximately 1.5. The average acceleration in both ranges was about 7g.

Flutter Wings

The four flutter wings were constructed of laminated maple and were made as nearly identical structurally as possible. The two wings of model 606 had the quarter-chord line swept back 45°, an aspect ratio of 8.01, a taper ratio of 0.54, and an NACA 65A009 airfoil section in the free-stream direction. The two wings of model 607 were the same as those of model 606 except that the quarter-chord line was rotated to 60° sweepback resulting in an aspect ratio of 4.25 and a free-stream thickness ratio of approximately 6.3 percent. Parameters of the wings which did not vary along the length are listed in table I and parameters which varied along the length are listed in table II. The tip station (station 9) was taken at the intersection of the quarter-chord line and the tip. The increment of the length between stations was 4 inches. All chordwise measurements were made perpendicular to the quarter-chord line.

Since for a swept wing there is no elastic axis in the commonly accepted sense of the term the values given in table I are an average, in the lengthwise direction, of the values determined for the flexural centers. The flexural center, as determined for spanwise stations 1 through 8, is the chordwise point of the station under consideration where a point load may be applied normal to the plane of the wing without causing rotation of the loaded station in the plane normal to the

quarter-chord line of the wing. The variation in these values amounted to about 5 percent of the wing chord.

Instrumentation and Test Procedure

A nine-channel telemeter was installed in each model and was designed to give continuous indications of the wing bending and torsional oscillations by use of strain gages mounted near the roots of the wing. The strain-gage patches may be seen in figure 2. Longitudinal acceleration, normal acceleration at the model center of gravity, total pressure, static pressure, and the angle of attack of the models were also transmitted continuously.

Velocity of the models was obtained by a continuous-wave Doppler velocimeter radar and the flight paths were obtained by reduction of data from a pulse-type tracking radar. Atmospheric conditions prevailing at the time of the flights were obtained from radiosondes. The flights of the models were recorded during the early stages by motion-picture cameras located near the launching area.

The models were launched at the Langley Pilotless Aircraft Research Station, Wallops Island, Va.

RESULTS AND DISCUSSION

Experimental results and the calculated flutter speeds and frequencies for the two pairs of wings are presented in table III. Figure 3 shows the variation of velocity, Mach number, and density with time for each of the models.

The 45° swept wings fluttered at a Mach number of 0.89 (982 feet per second), continued to flutter through the maximum speed attained in the test (1292 feet per second, $M = 1.175$) and stopped fluttering at a Mach number of 0.84 (926 feet per second). There is no indication that either wing failed. The 60° swept wings fluttered at a Mach number of 1.09 (1208 feet per second), continued to flutter through the maximum speed attained in the test (1663 feet per second, $M = 1.52$), and stopped fluttering at a Mach number of 1.03 (1132 feet per second). At the maximum speed of the test of model 607, the flutter had decreased considerably in amplitude from the initial value which leads to the belief that the model nearly passed from a range of Mach numbers in which the wing fluttered to a higher Mach number range where no flutter would occur. That portion of the telemeter record on which are recorded the signals from the right wing bending and torsion gages, total pressure, and static pressure is shown in figure 4. The decrease in amplitude may

be seen by comparing the strain-gage traces at 4 seconds to those at the maximum velocity of the test, 5.7 seconds.

The records of normal acceleration of the two models show a maximum acceleration of the model center of gravity of approximately ±5g which is equivalent, at the flutter frequency, to a vertical translation of about ±0.01 inch. Immediately prior to flutter, the angle of attack was 0.35°. It is felt that body motion and angle of attack of this order of magnitude would have no appreciable effect on the flutter of these wings.

In order that the results may be readily compared with previous tests, a theoretical, or reference, flutter speed V_R was calculated by the method of reference 4; that is to say on the basis of two-dimensional flow (strip analysis), with calculated mode shapes (Rayleigh-Ritz procedure) and with account taken of the angle of sweep. Aerodynamic coefficients for two-dimensional incompressible flow were employed in conjunction with two degrees of freedom. The mode shapes were those of first bending and first torsion of a tapered cantilever beam, calculated from the known stiffness, mass, and inertia properties of the wings. The frequencies used were the uncoupled first-bending and first-torsional frequencies, respectively, for each wing. The density used was the density at which flutter started.

With reference to the effect of aspect ratio it may be pertinent to note at this point that in reference 1 it was reported that no flutter occurred up to a maximum test Mach number of 1.45 in the tests of a pair of 45° swept wings (A = 3.93) and a pair of 60° swept wings (A = 2.16). Flutter did occur in the tests of models 606 and 607 (A = 8.01 and 4.25, respectively) at Mach numbers considerably less than 1.45 even though the reference flutter speeds of the wings of models 606 and 607 are slightly higher than those calculated for the wings of corresponding sweep reported in reference 1. Since the wings reported herein and the wings reported in reference 1 are quite similar except in aspect ratio, the differing experimental results are felt to be due to the effects of aspect ratio.

Figure 5, which is a plot of V/V_R and V_e/V_R against Mach number, presents the pertinent flutter data obtained in this investigation and also some data from previous investigations of straight wings (shown by the solid curve) for comparison purposes. With reference first to the present tests, the flutter trace depicting the Mach number range through which the models flutter is shown by the cross-hatched areas. It can be seen from the figure that the speed at the beginning of flutter V_e and the reference flutter speed V_R compare very well for both models. For model 606 (45° sweep) the ratio V_e/V_R was 1.053 for the left wing and 1.011 for the right. For model 607 (60° sweep) the ratio was 1.029 for

the left wing and 1.020 for the right. Such excellent agreement is not to be expected in every case and must be considered partly fortuitous; nevertheless it indicates that the method of calculation utilized provides usable results in the transonic region. This method involves the use of flutter derivatives for two-dimensional, incompressible flow normal to the wing and includes effects of sweep and mode shape.

The two curves shown in figure 5 are flutter boundary lines. The solid curve is a composite experimental flutter curve for untapered, unswept wings, taken from figure 6 of reference 5. The dashed curve is an estimated flutter curve for the 60° swept wing drawn by using the points of the beginning of flutter of the tests reported herein and by enveloping the region of flutter by a curve approximating the shape of the curve for the unswept wings. The swept and unswept wings from which the data were obtained have about the same aspect ratio (high) and center-section-of-gravity location; therefore, a comparison of the two sets of data should indicate the effects of sweep in the transonic region. As may be seen from a comparison of the solid and the dashed curves, the supersonic flutter-free region for the swept wings, indicated by the turn-up of the dashed curve, lies, as suggested in reference 6, at a higher Mach number than for the unswept wings.

CONCLUDING REMARKS

Flutter has been obtained in the transonic range with two pairs of high-aspect-ratio swept wings at speeds which are in good agreement with those calculated by incompressible-flow theory. The indication is that the use of incompressible two-dimensional-flow flutter derivatives based on flow normal to the wing is valid in the transonic speed range for swept wings of high aspect ratio provided that the normal flow Mach number is sufficiently subsonic. There is the further indication that the turn-up of the experimental flutter curve presented in NACA RM L9B25b is moved to a higher Mach number range for swept wings of relatively high aspect ratio.

Langley Aeronautical Laboratory
National Advisory Committee for Aeronautics
Langley Field, Va.

[redacted]

REFERENCES

1. Lauten, William T., Jr., and Teitelbaum, J. M.: Some Experiments on the Flutter of Wings With Sweepback in the Transonic Speed Range Utilizing Rocket-Propelled Vehicles. NACA RM L50C03a, 1950.

2. Lauten, W. T., Jr., and Sylvester, Maurice A.: Flutter Investigation of a Pair of Thin, Low-Aspect-Ratio, Swept, Solid, Metal Wings in the Transonic Range by Use of a Free-Falling Body. NACA RM L51K28a, 1952.

3. Tuovila, W. J.: Some Experiments on the Flutter of Sweptback Cantilever Wing Models at Mach Number 1.3. NACA RM L51A11, 1951.

4. Barmby, J. G., Cunningham, H. J., and Garrick, I. E.: Study of Effects of Sweep on the Flutter of Cantilever Wings. NACA Rep. 1014, 1951. (Supersedes NACA TN 2121.)

5. Lauten, William T., Jr., and Barmby, J. G.: Continuation of Wing Flutter Investigation in the Transonic Range and Presentation of a Limited Summary of Flutter Data. NACA RM L9B25b, 1949.

6. Regier, Arthur A., and Martin, Dennis J.: Recent Experimental Flutter Studies. NACA RM L51F11, 1951.

[redacted]

TABLE I

CONSTANT WING PARAMETERS

Parameter	Wing			
	606 Left	606 Right	607 Left	607 Right
l, in.	38.75	38.75	37.5	37.5
A	8.01	8.01	4.25	4.25
x_1, percent chord	44.05	44.05	44.05	44.05
x_o, percent chord	64.75	58.70	67.89	59.74
a	0.295	0.174	0.358	0.195
$a + x_\alpha$	-0.119	-0.119	-0.119	-0.119
*μ	64.1	70.5	58.5	59.3
r_α^2	0.424	0.3395	0.4812	0.3516
f_{h_1}, cps	16.5	17.0	18.0	21.0
f_{h_2}, cps	74.0	74.5	76.0	89.0
f_{α_1}, cps	109.4	119.8	115.5	117.3
Λ, deg	45	45	60	60
λ	0.54	0.54	0.54	0.54

*At standard conditions.

NACA

TABLE II

SPANWISE VARIATION OF WING PARAMETERS

[Applies to all wings]

Station	b (ft)	F_{h_1}	F_{α_1}	Fraction of span
0	0.287	0	0	0
1	.273	.014	.107	.111
2	.259	.056	.230	.222
3	.245	.127	.365	.333
4	.231	.225	.506	.444
5	.217	.349	.647	.555
6	.203	.493	.777	.667
7	.189	.656	.890	.778
8	.175	.826	.969	.889
9	.161	1.000	1.000	1.000

NACA

[redacted]

TABLE III

EXPERIMENTAL FLUTTER DATA

Parameter	Wing			
	606 Left	606 Right	607 Left	607 Right
M_e	0.89	0.89	1.09	1.09
V_e, fps	982	982	1208	1208
f_e, cps	64	64	59	59
ρ_e, slug/cu ft	0.00214	0.00214	0.002353	0.002353
q, lb/sq ft	1074	1074	1717	1717
μ_e	71.25	78.40	59.17	59.98
V_R, fps	933	971	1174	1184
f_R, cps	60.8	62.4	63.1	60.8
V_e/V_R	1.053	1.011	1.029	1.020

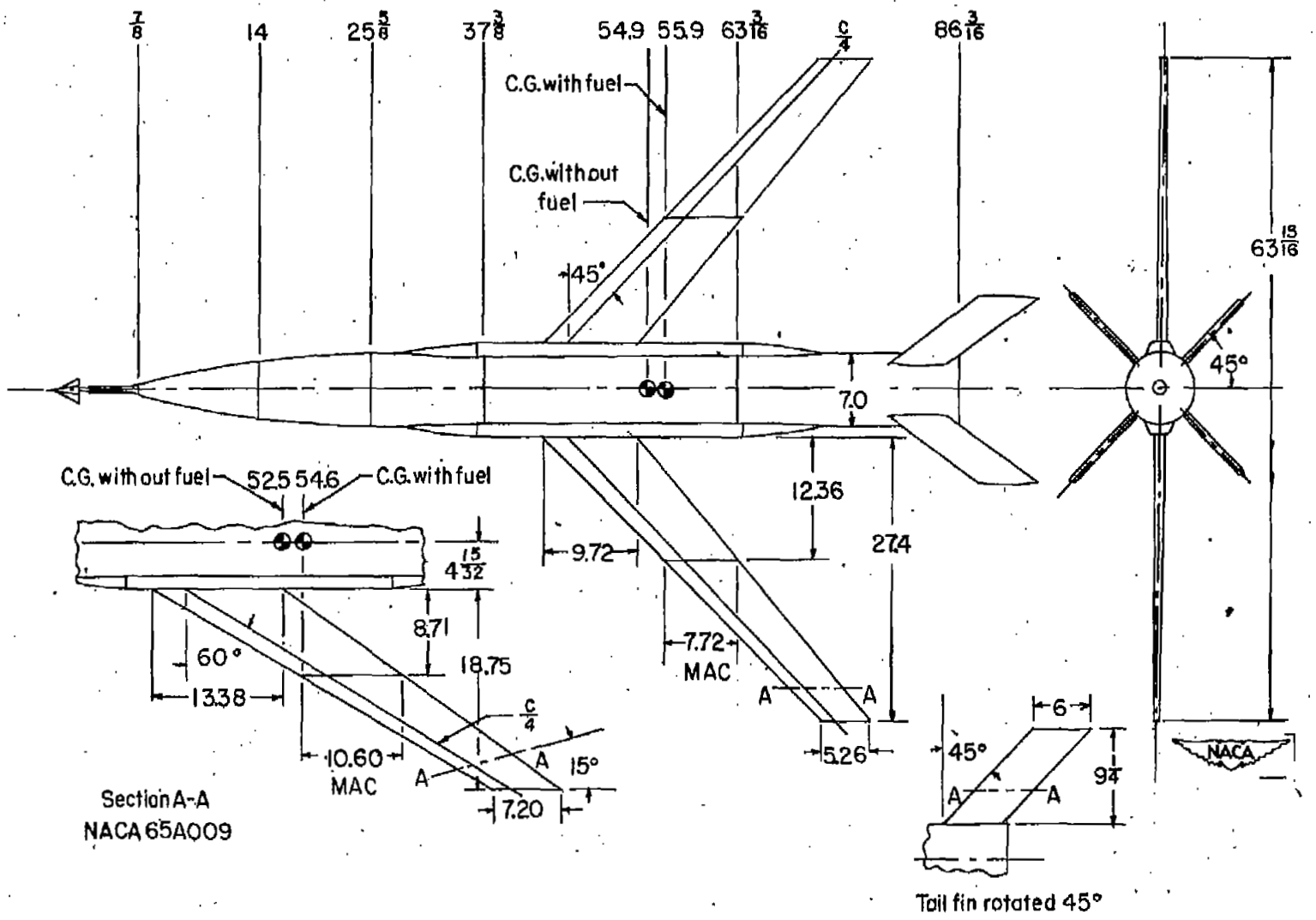

Figure 1.- Sketch of flutter test vehicle. All dimensions are in inches.

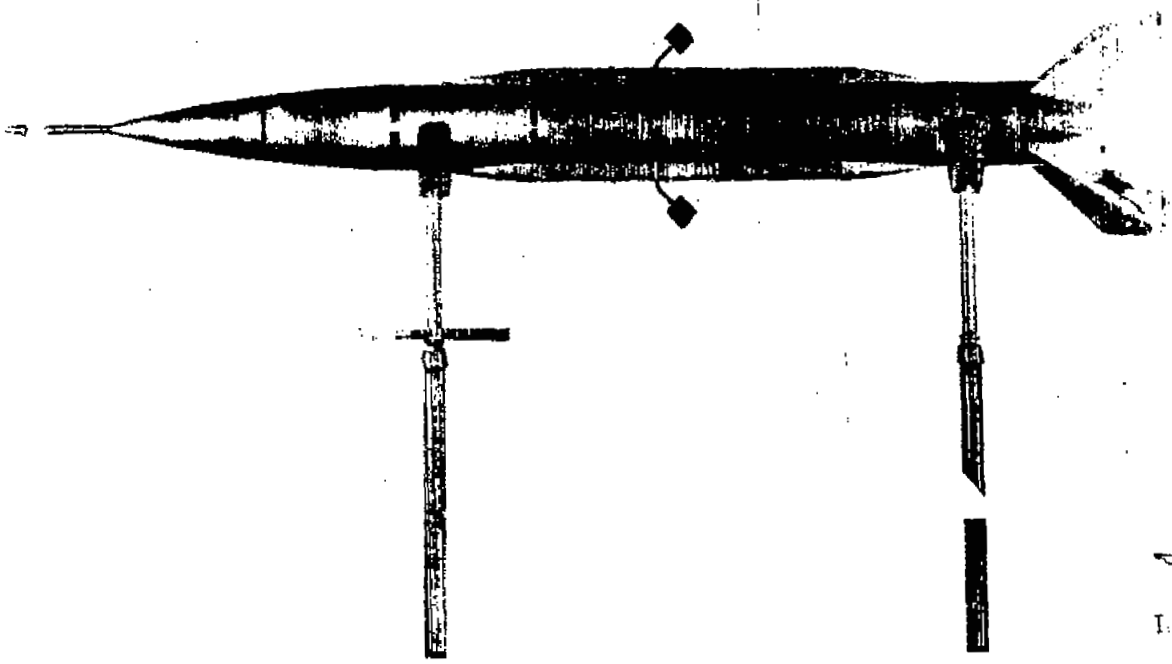

NACA
L-68[illegible].1
12/50

(a) Top view of model 606.

Figure 2.- Laboratory photographs of models.

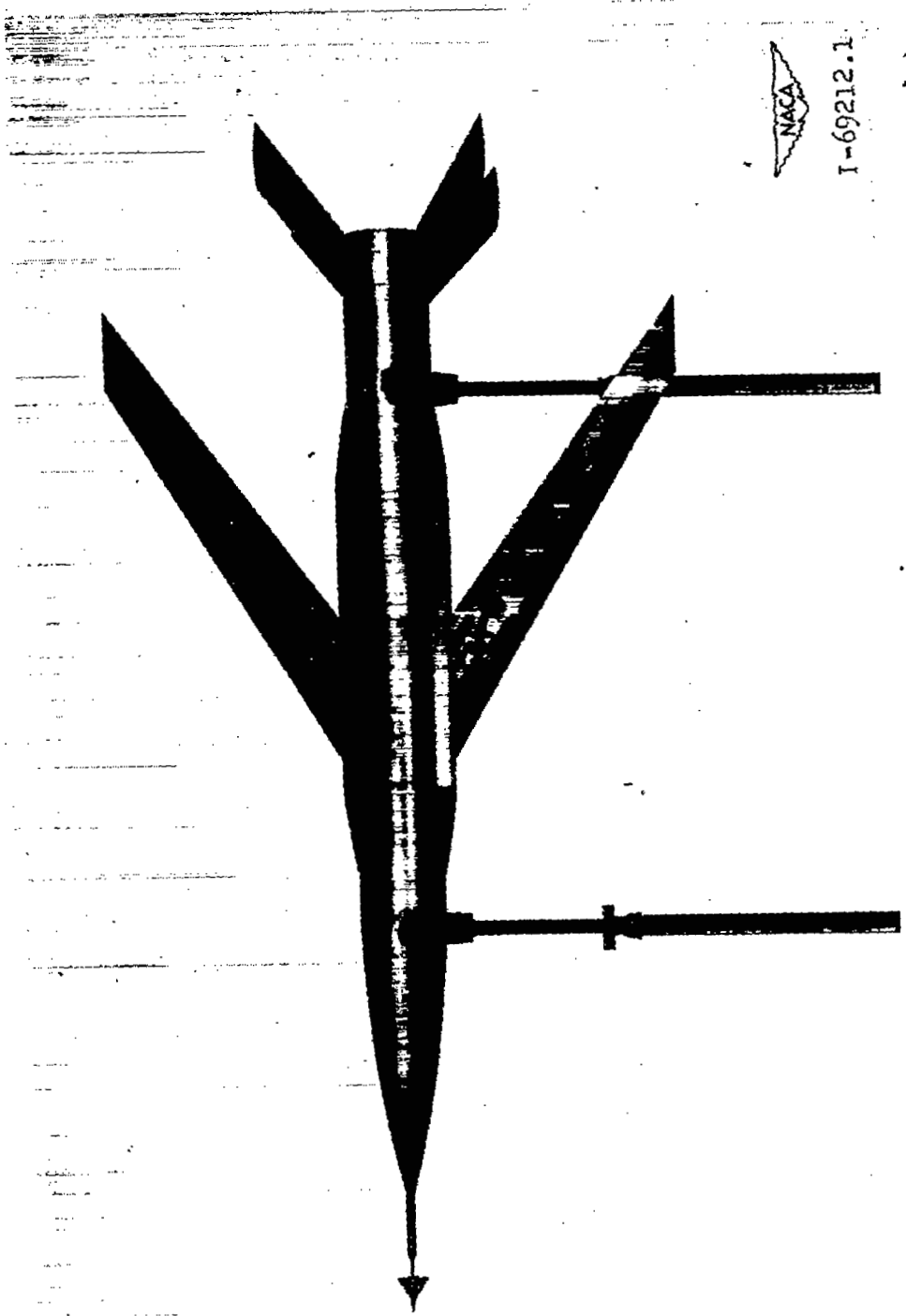

I-69212.1

(b) Top view of model 607.

Figure 2.- Continued.

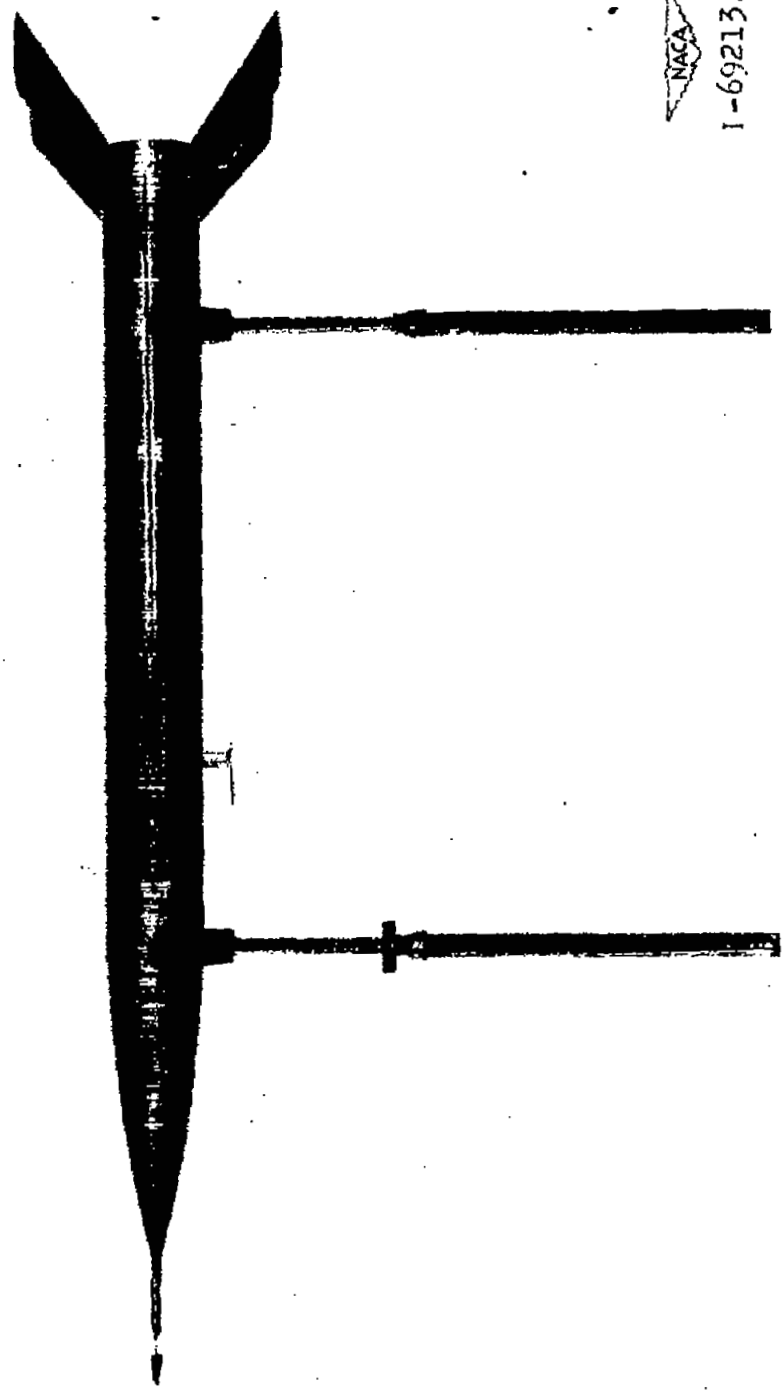

NACA L-69213.1

(c) Side view of model 607.

Figure 2.- Concluded.

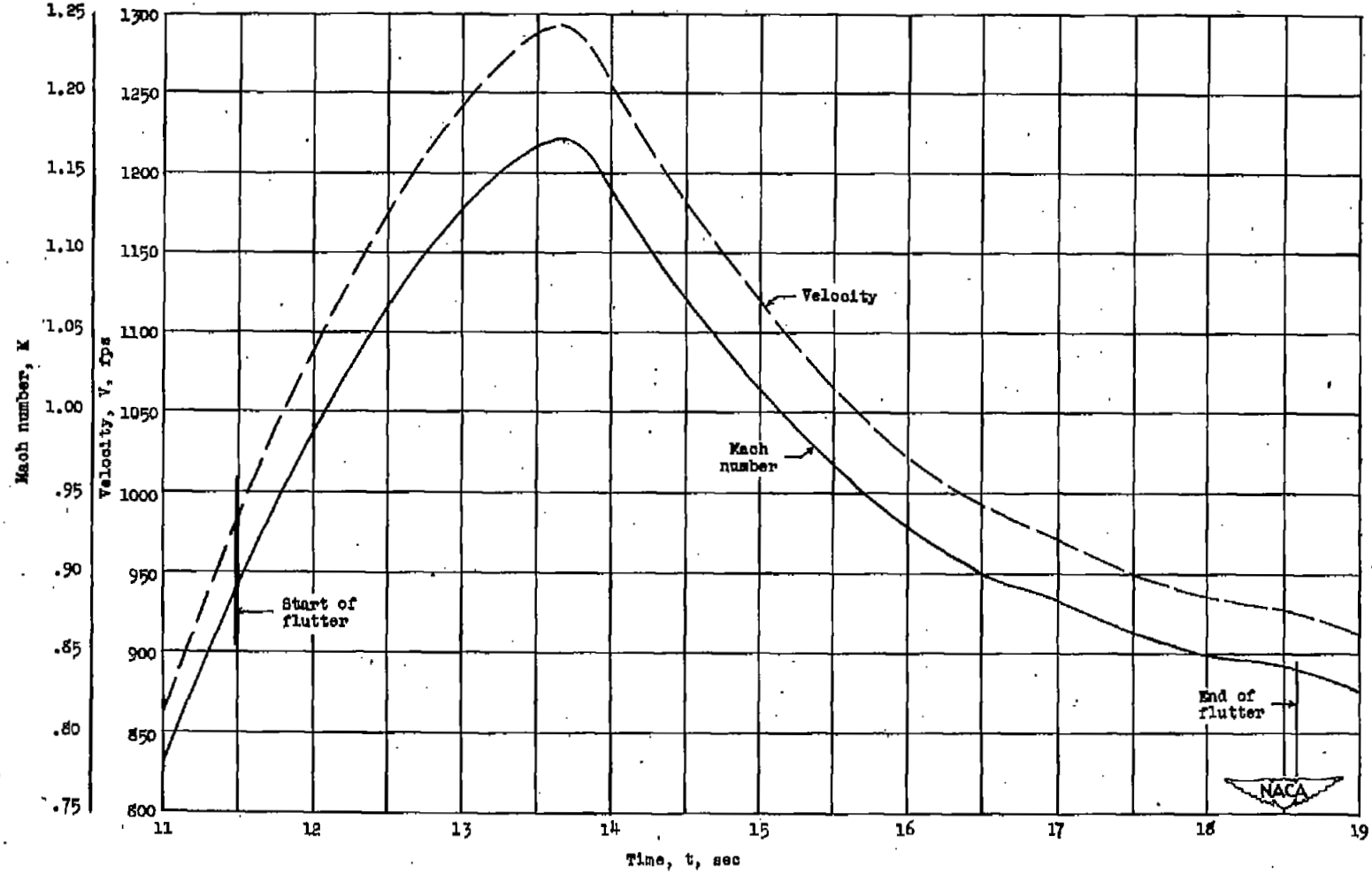

(a) Variation of velocity and Mach number for model 606.

Figure 3.- Variation of velocity, Mach number, and air density with time for models 606 and 607.

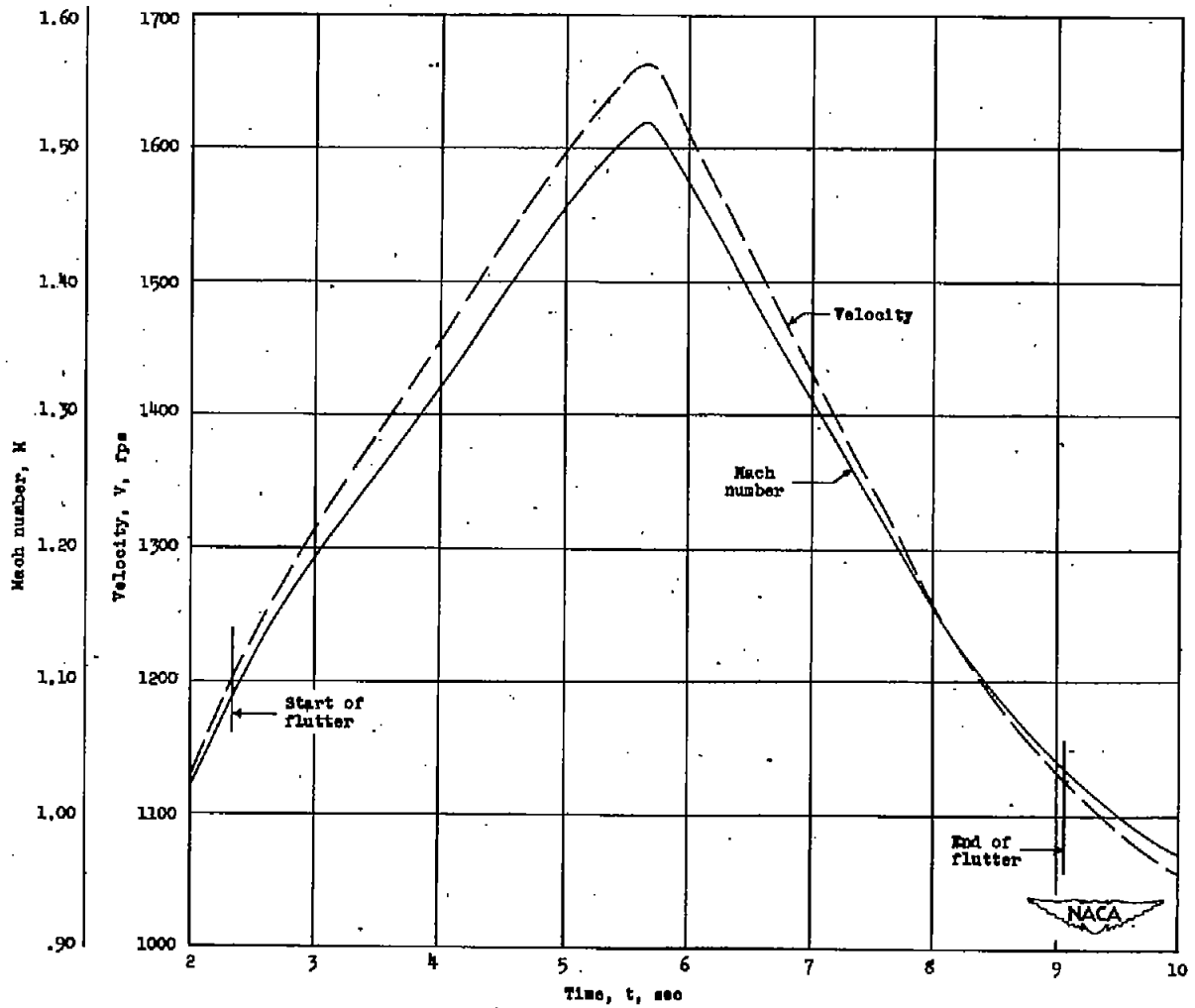

(b) Variation of velocity and Mach number for model 607.

Figure 3.- Continued.

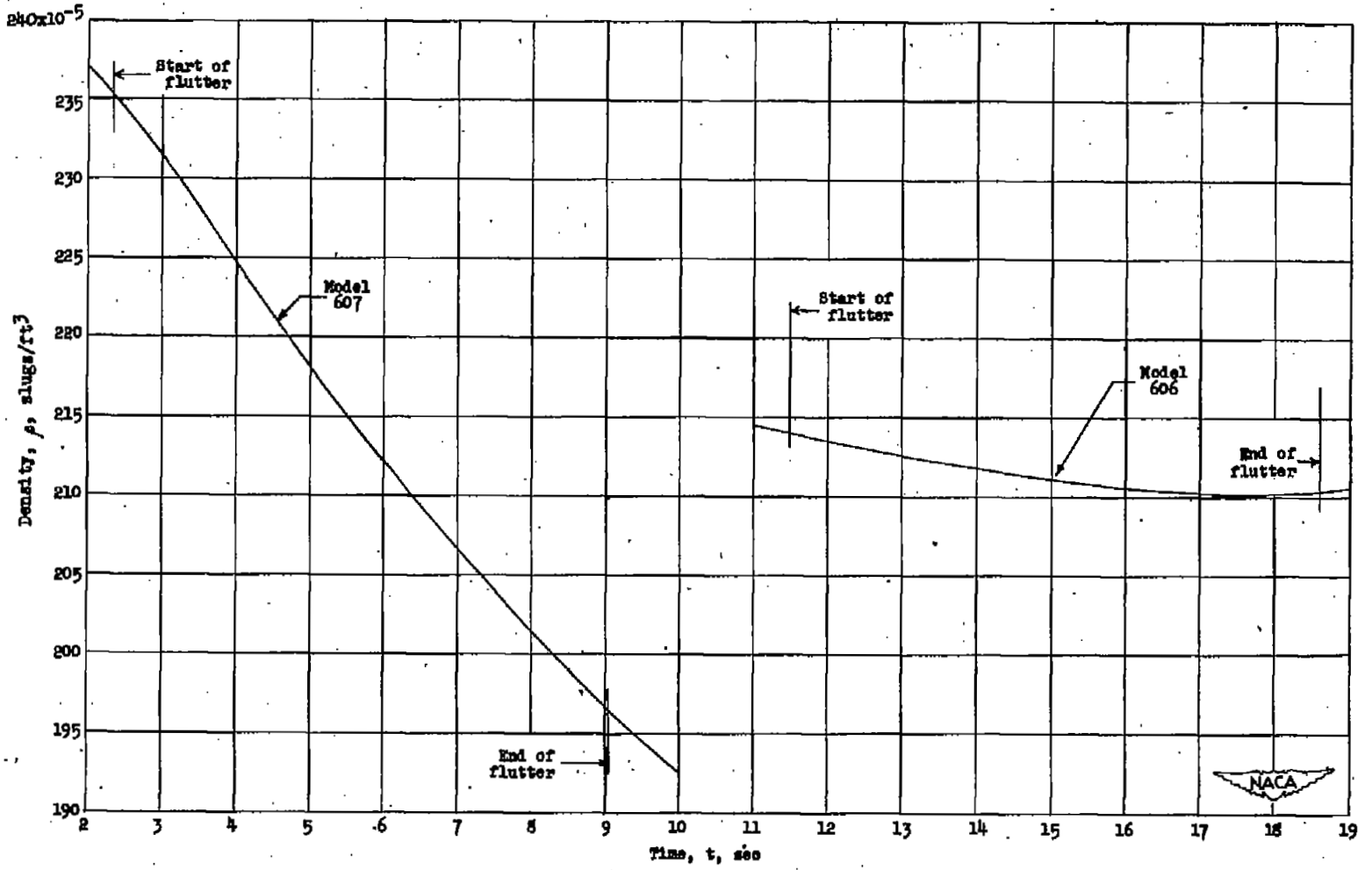

(c) Variation of air density for models 606 and 607.

Figure 3.- Concluded.

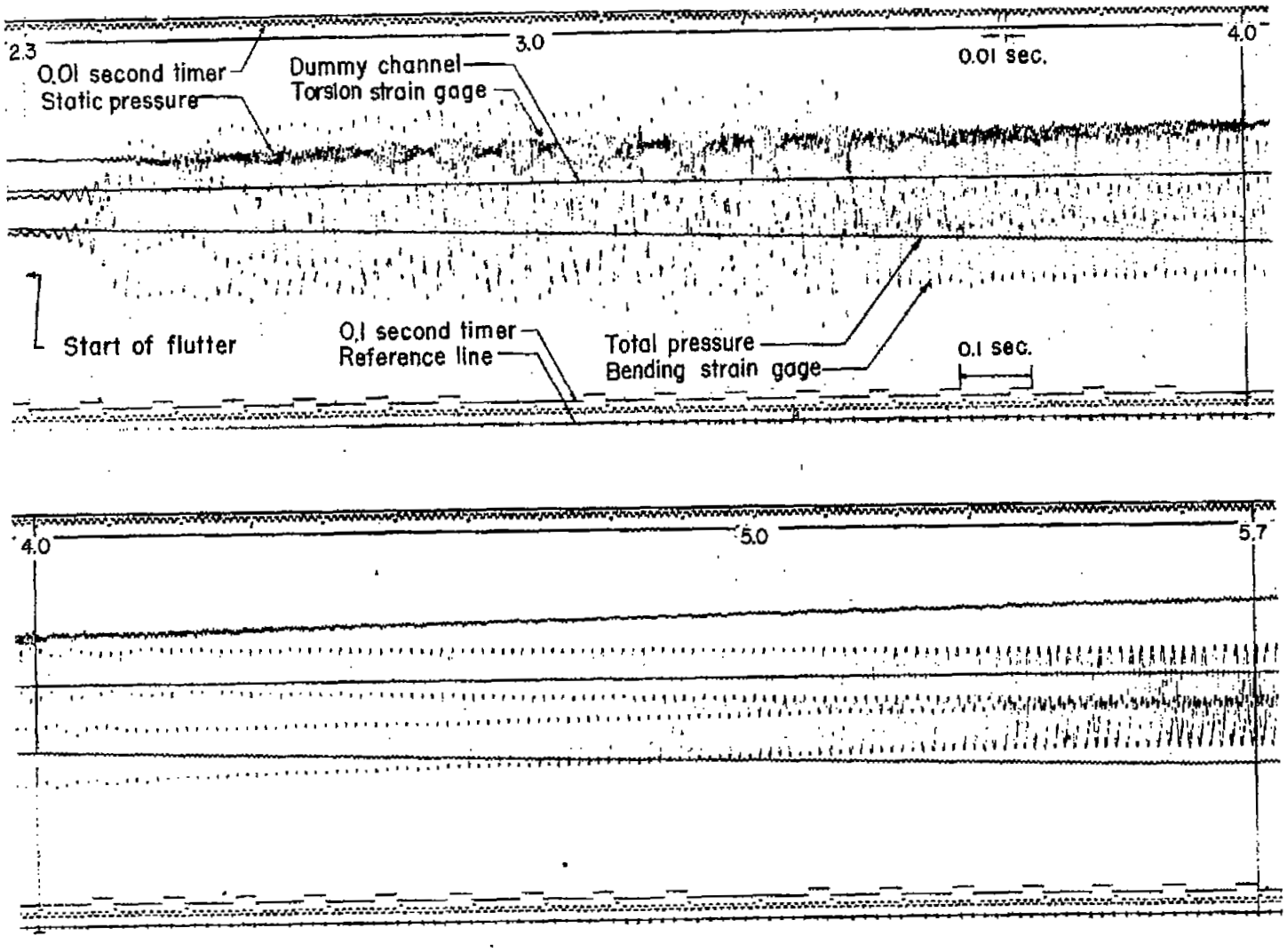

Figure 4.- Flutter record of model 607.

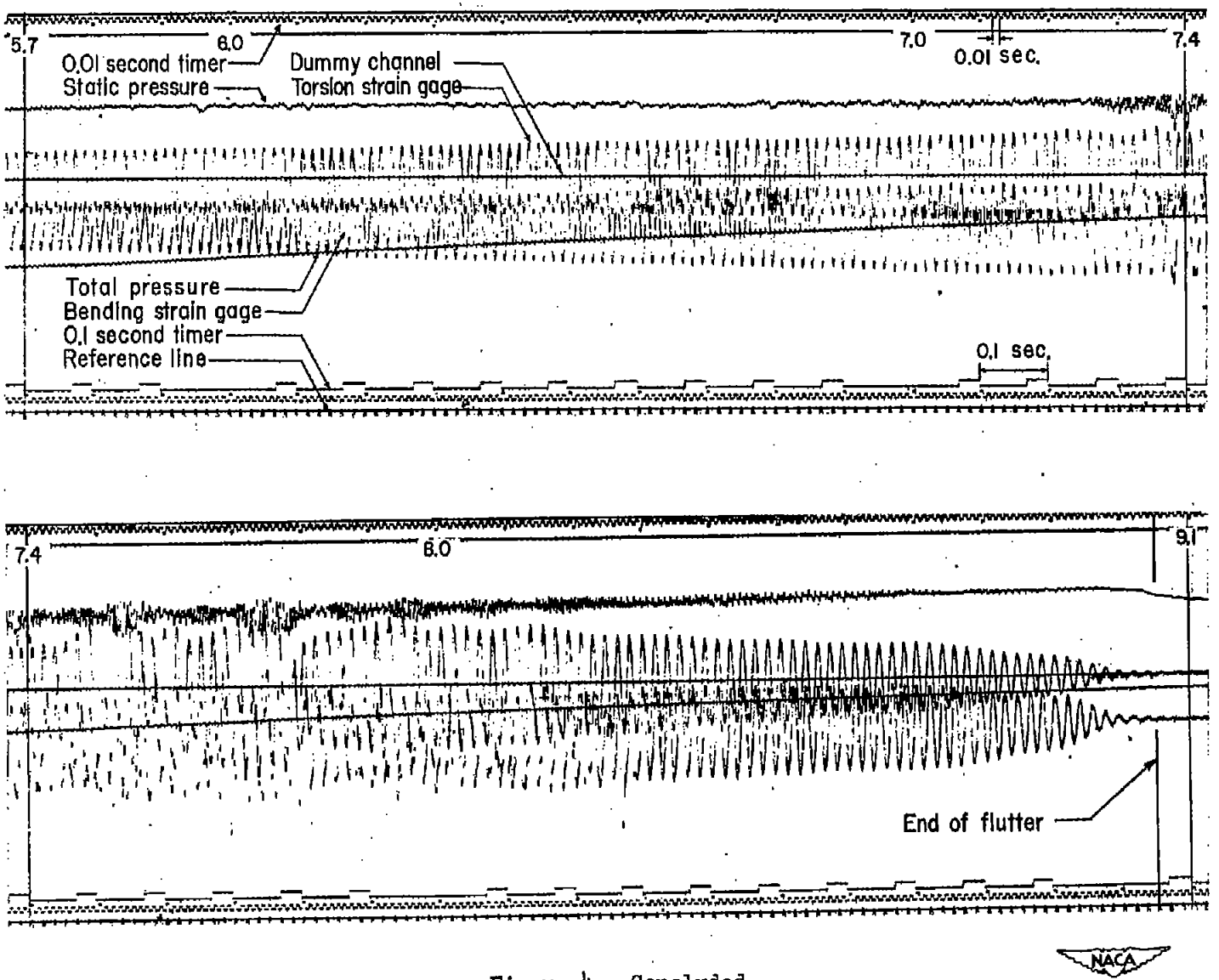

Figure 4.- Concluded.

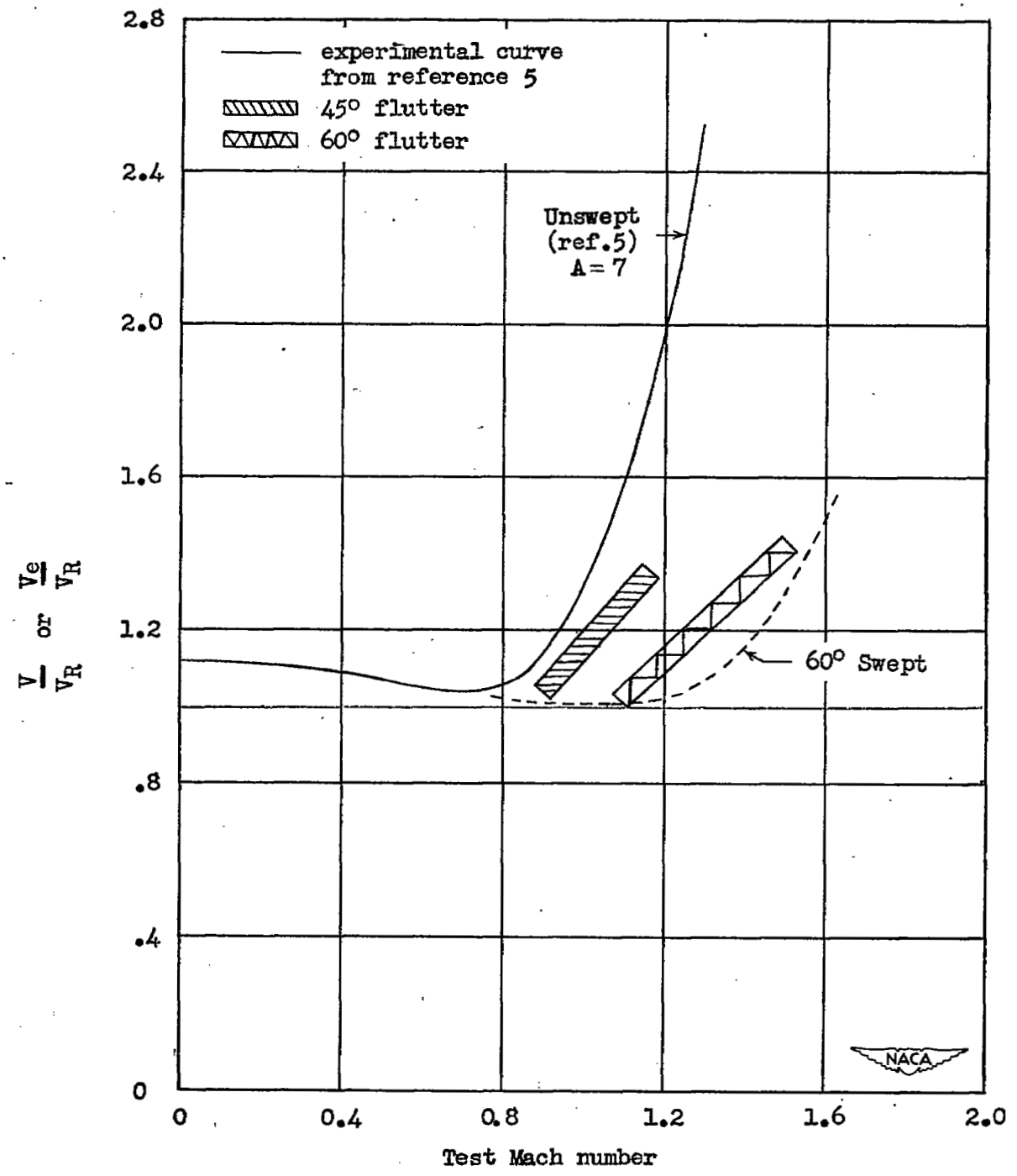

Figure 5.- $\frac{V}{V_R}$ and $\frac{V_e}{V_R}$ plotted as a function of Mach number.

[redacted]

SECURITY INFORMATION

[redacted]